Toward Controlled Donor−Acceptor Interactions in Noncomposite Polymeric Materials: Synthesis and Characterization of a Novel Polythiophene Incorporating π-Conjugated 1,3-Dithiole-2-ylidenefluorene Units as Strong D−A Components

Peter J. Skabara* and Igor M. Serebryakov

Materials Research Institute, Sheffield Hallam University, Sheffield S1 1WB, U.K.

Igor F. Perepichka

L. M. Litvinenko Institute of Physical Organic and Coal Chemistry, National Academy of Sciences of Ukraine, Donetsk 83114, Ukraine

N. Serdar Sariciftci, Helmut Neugebauer, and Antonio Cravino

Linz Institute for Organic Solar Cells (LIOS), Physical Chemistry, Johannes Kepler University Linz, A-4040, Austria

Received September 14, 2000; Revised Manuscript Received December 19, 2000

ABSTRACT: A novel polythiophene bearing a strong electron-accepting fluorene unit has been synthesized. Poly(**2d**) can be prepared by chemical (iron(III) chloride) or electrochemical oxidation. Intramolecular charge-transfer (ICT) within the polymer was studied by electronic absorption spectroscopy and compared to a series of model monomer derivatives. The redox properties of the materials were studied by cyclic voltammetry; polythiophene main chain in poly(**2d**) is oxidized at ca. +0.7 V vs Ag/AgCl, while the nitrofluorene repeat unit is reduced at ca. −0.5 and −0.7 V. The model compounds **3a**−**e** show a Hammett-type correlation for ICT energies, $E_{1red}^{1/2}$ and $E_{2red}^{1/2}$ vs the substituents on the fluorene ring, with the sensitivity parameters $\rho_{ICT^-} \approx 0.17-0.20$ eV and $\rho_{CV^-} \approx 0.17-0.25$ V. In contrast, the oxidation process (E_{ox}) displays very low sensitivity to the structure of the fluorene ring ($\rho_{CV^-} \approx 0.04$ V), indicating that ICT can be substantially tuned without a noticeable effect on the redox properties of the thiophene moiety in **3**; this behavior can be extended (extrapolated) to terthiophenes **2** and their polymers. Photoinduced IR spectroscopy of poly(**2d**) provides evidence of long-living photoexcited charge transfer in the polymer.

Introduction

Substituted fluorenes are compounds which offer a wide range of π-electron-accepting ability, relative to the electron-withdrawing power and number of substituents.[1] Thus, for example, charge-transfer (CT) materials have been obtained from the complexation of unsubstituted fluorene with the highly efficient acceptor TCNQ[2] and 9-substituted polynitrofluorenes with the strong π-electron donor TTF.[1,3]

Because of the acidic nature of the protons at C-9, fluorene derivatives are able to undergo condensation reactions with suitable electrophiles, leading to substitution at the 9-position via a C−C double bond. Using this strategy, several classes of donor−acceptor π-conjugated derivatives have been prepared.[4−8] These compounds show long-wavelength absorption bands in the visible/near IR region of their electronic spectra, arising from an intramolecular charge-transfer (ICT) process. The propensity for electron deficient fluorene derivatives to form stable CT complexes has been utilized in the sensitization of carbazole-based polymers toward photoconductivity.[9] Moreover, it has been shown recently that fluorenes exhibiting ICT possess drastically increased photosensitizing effects which correlate within their ICT spectral parameters.[5,6,7b,10] This feature provides a route toward the precise control in spectral response of the photosensitivity, since the value of λ_{ICT}^{max} is totally dependent upon the summative electron-withdrawing ability of the fluorene ring substituents.[4,5,8,11]

Recently, we reported the synthesis of a range of thieno-1,3-dithiole-2-ylidenefluorene monomers based on **1**.[4] The substituents on the fluorene ring system (W, X, Y, Z = H, NO_2, or CO_2R) dictate the electron-accepting ability of the molecule, whereas the central 1,3-dithiole ring acts as a π-resonance donor, complementary to the fluorene unit. We have thoroughly investigated the electrochemical and intramolecular charge-transfer properties of these systems and have found that the reduction potentials and ICT are highly dependent upon the sum of the Hammett-type constants of the substituents.[4] Thus, we have shown that these monomers can be tuned synthetically to give predictable levels of electroactivity. This information can be used in the development of fluorene-bearing polymers to give materials with a range of desired electronic properties.

The study of photoinduced electron transfer (PET) in processable materials (e.g., conjugated oligomers/polymers and C_{60} composites), represents an area of high interest with the following potential applications:[12] NLO devices, cost-effective organic solar cells, photodiodes with an infrared response and even photoinduced superconductivity. The current state-of-the-art in photoconducting materials, based on conjugated polymers (CPs), involves the use of polymer−acceptor composites (e.g., soluble PPV−C_{60}). Upon photoexcitation, it is

* To whom correspondence should be addressed. New address: Department of Chemistry, University of Manchester, Manchester M13 9PL, U.K. E-mail: Peter.Skabara@man.ac.uk.

10.1021/ma0015931 CCC: $20.00
Published on Web 03/03/2001

desirable that the charge separated states are formed in the picosecond range and are long-lived[13] and do not undergo immediate charge back-transfer; therefore, it is notable that PET in C_{60}-containing donor−acceptor (D−A) composites and D-σ-A and D-π-A molecules has been shown to give long-lived charge-separated states.[14] However, a vast range of π-acceptor molecules are known, which are readily available and could be used as preferred redox species to C_{60}, particularly from preparative, cost-efficient, and tunable viewpoints.

Specifically, fluorene-containing CPs from monomers **1** would have the following advantages over composite polymer−acceptor materials: (i) a totally homogeneous structure; (ii) a known, fixed donor−acceptor ratio; (iii) a precise distance between the acceptor unit and the polymer chain; (iv) in a bilayer device, efficient charge-separation only taking place at the donor−acceptor interface but, in the bulk material, the photoexcitation recombining prior to diffusion to the D/A junction. On the other hand, composite layers provide a high interfacial area; however, this arrangement is still inferior to donor−acceptor polymers of the type poly(**1**).

In our attempts to polymerize the fluorene monomers **1** via electrochemical oxidation, we believe that the resulting radical cations predominate within the 1,3-dithiole fragment of the monomer, thereby eliminating the possibility of coupling between the thiophene units. Furthermore, steric hindrance from the approaching fluorene units would render any dimerization process highly unlikely. To this end, we have prepared the terthiophene derivatives **2**, which are convenient precursors to polythiophene copolymers. The extended chain of the terthiophene reduces the adversity of steric hindrance from substituents on the central ring, while the cation radical intermediate obtained by oxidation will be affected less by the electronic behavior of the 1,3-dithiole unit, due to the fused 1,4-dithiino spacer group. Using this approach, we have succeeded in the preparation and electrochemical polymerization of fluorene derivative **2d**, which has been the subject of a preliminary communication.[15]

Herein, we describe the preparation of terthiophenes **2b**,**d**,**e**, together with their ICT and electrochemical properties. The model compounds **3a**−**e** have also been synthesized and fully characterized, to check the contribution (if any) of the 1,4-dithiino ring, which is absent in series **1**. In addition, we detail the polymerization (chemical and electrochemical) of **2d**. Poly(**2d**) has been investigated by in situ FTIR spectroscopy during electrochemical oxidation. Finally, the nature of the photoexcited states has been studied by photoinduced FTIR absorption.

Results and Discussion

Synthesis. Compounds **3a**−**e** were prepared by the condensation of substituted fluorenes **6a**−**e**[4,16,17] with the dithiolium salt **5** (25−78% yield, Scheme 1), which in turn was obtained by methylation of thione **4** with methyl trifluoromethanesulfonate (53% yield). The most obvious route to the key intermediate **4** seemed to be the one-step condensation of 3,4-dibromothiophene with 1,3-dithiolo-2-thione-4,5-dithiolate (DMIT). However, in the presence of classical Cu(I) catalysts, the analogous process requires vigorous conditions (130−140 °C, 24 h),[18] under which DMIT itself is unstable.[19] The use of palladium(0) or nickel(0) triphenylphosphine complexes as catalysts allows one to carry out the reactions of aryl halides with thiols at 50−100 °C.[20,21] However, our attempt at coupling the cesium salt of DMIT[19] with 3,4-dibromothiophene under phase-transfer conditions,[21] even in the presence of an equimolar amount of Pd-

Chart 1

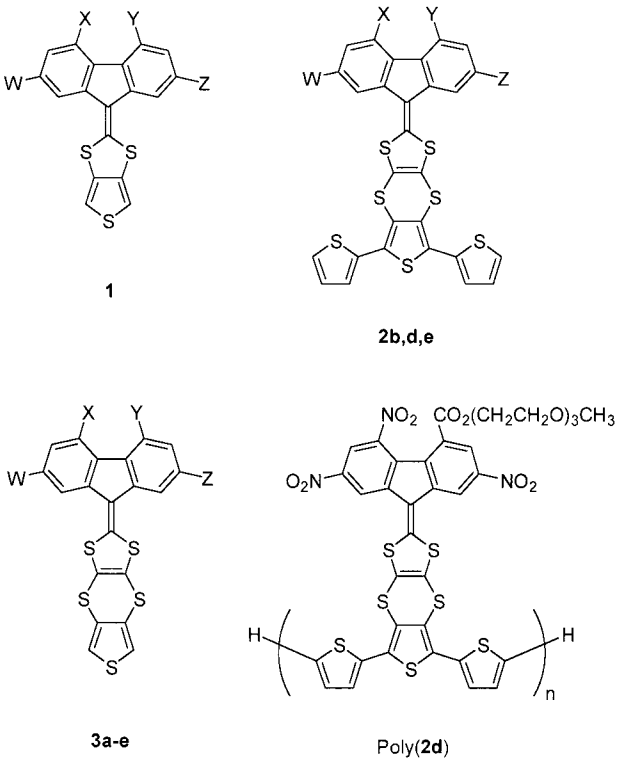

	W	X	Y	Z
a	NO_2	H	H	NO_2
b	NO_2	H	$CO_2(CH_2CH_2O)_3CH_2CH_3$	NO_2
c	NO_2	NO_2	H	NO_2
d	NO_2	NO_2	$CO_2(CH_2CH_2O)_3CH_3$	NO_2
e	NO_2	NO_2	NO_2	NO_2

Scheme 1[a]

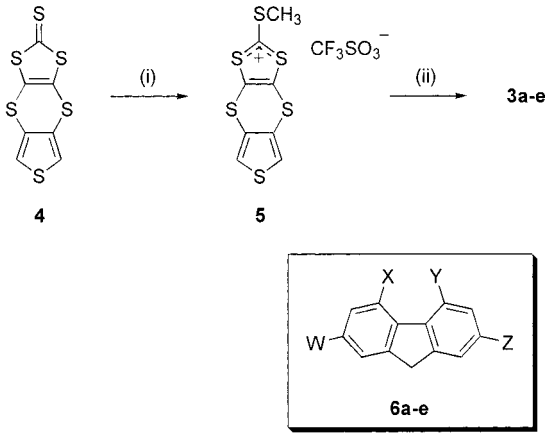

[a] Reagents and conditions: (i) $CF_3SO_3CH_3$, CH_2Cl_2, 20 °C, 16 h; (ii) **6a**−**e**, pyridine or DMF, 60−90 °C, 15−30 min.

Scheme 2[a]

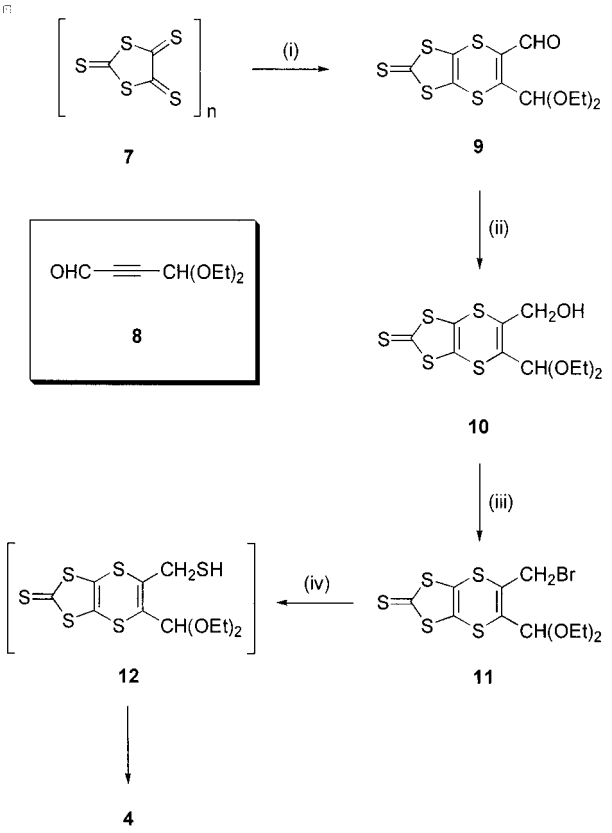

[a] Reagents and conditions: (i) **8**, toluene, 2,6-lutidine, 70 °C, 45 min; (ii) $NaBH_4$, THF, room temperature, 2 min; (iii) PPh_3, CBr_4, THF, 2,6-lutidine, room temperature, 40 min; (iv) NaSH, MeOH, THF, −20 °C, 2.5 min, and then HCl, room temperature to 50 °C.

$(PPh_3)_4$, produced a mixture of triphenylphosphine and probably triphenylphosphine sulfide (EIMS $m/z = 294$), along with the majority of unchanged starting material 3,4-dibromothiophene.

A successful approach to the synthesis of **4** is depicted in Scheme 2. In the presence of 2,6-lutidine, the Diels−Alder condensation of oligomer **7**[22] with the diethylacetal of acetylene dicarboxaldehyde **8**[23] gave dithiin **9**[24] in 48% yield. Reduction of the aldehyde group with $NaBH_4$ in tetrahydrofuran (THF) proceeded smoothly to give alcohol **10** (98% yield). The conversion of **10** to the bromo derivative **11** (63%) required the addition of a hindered base (2,6-lutidine) to the standard reagents PPh_3 and CBr_4. Compound **11** was converted to the thiophene derivative **4** by treatment with a large excess of sodium hydrogen sulfide, involving in situ deprotection of the aldehyde group in the intermediate mercaptan **12**.

Compounds **2b**,**d**,**e** were prepared according to Scheme 3 (40−50% yield) by the condensation of substituted fluorenes **6b**,**d**,**e**,[4,17] with dithiolium salt **14**, which in turn was obtained by the methylation of thione **13**[25] with methyl trifluoromethanesulfonate. The alkylation procedure required a larger excess of methyl triflate and a longer reaction time, compared with the related thione **4**, mainly due to the low solubility of terthiophene **13**. Salt **14** was readily soluble in dichloromethane (DCM), but precipitated on addition of dry diethyl ether as a green tarry residue; because of the instability of the material **14** was used in the subsequent step without further purification. During our studies, we also prepared the corresponding derivatives of di- and trinitrofluorenes (**2a** and **2c**), but their solubility was too low to purify them by recrystallization or to investigate their redox properties.

Scheme 3[a]

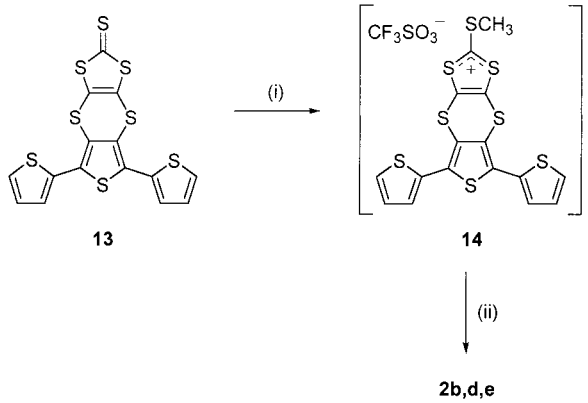

[a] Reagents and conditions: (i) CF_3SO_3Me, DCM, 3 d, and then (ii) **6b**,**d**,**e**, pyridine or DMF, 80−90 °C, 30 min.

Absorption Spectroscopy. Electronic absorption studies were performed on compounds **2b**,**d**,**e** and **3a**−**e** in DMF; the longest wavelength maxima, corresponding to ICT, are collated in Table 1. As expected, the values for λ_{ICT}^{max} are shifted bathochromically with an increase in the sum of the nucleophilic constants σ_p^- attached to the fluorene ring. This trend can be expressed quantitatively by eq 1, from which the substituent sensitivity parameter (ρ^-) for the intramolecular charge-transfer bands can be calculated, where $h\nu_{ICT}$ is the ICT energy (in eV) corresponding to λ_{ICT}^{max} of each derivative, $\sum\sigma_p^-$ is the sum of the nucleophilic constants of the substituents[26] and $h\nu^0_{ICT}$ is the theoretical value corresponding to zero substituents on the fluorene system (i.e., $\sum\sigma_p^- = 0$).

$$h\nu_{ICT} = h\nu^0_{ICT} + \rho^-\sum\sigma_p^- \qquad (1)$$

The plot of $h\nu_{ICT}$ vs the sum of the nucleophilic constants is depicted in Figure 1. Both fluorene systems show very good linear relationships with correlation coefficients (r) greater than 0.99 (Table 2). The substituent sensitivity constants for compounds **2b**,**d**,**e** and **3a**−**e** are 0.20 V and 0.17 V, respectively, which are very close to the related series **1** (0.18 V).[4] It is evident, therefore, that the 1,4-dithiino spacer does not have a dramatic effect on the ICT processes in compounds **2** and **3**. Taking into account that these ρ^- values are also close to those for other 9-dithiolylidenefluorenes,[5,8,11] we conclude that ICT evolves mainly from the dithiole ring on the fluorene moiety and that the thiophene unit only has a slight effect on this process.

Cyclic Voltammetry. Electrochemical studies were performed on both thiophene (**3b**−**e**) and terthiophene (**2d**,**e**) derivatives in *N*,*N*-dimethylformamide (DMF) and dichloromethane (DCM) vs Ag/AgCl, using tetrabutylammonium hexafluorophosphate ($^nBu_4N^+PF_6^-$) as the supporting electrolyte; compounds **3a** and **2b** proved to be too insoluble to give reliable data. A typical cyclic voltammogram for the fluorene systems is represented in Figure 2, which shows the electroactivity of thiophene **3d** in DMF solution (the larger peak at ca. −0.75 V is due to the solvent). All compounds give a single irreversible peak between +1.28 and +1.39 V (Table 1), corresponding to the oxidation of the thiophene/

Table 1. Maxima of ICT Bands (λ_{ICT}^{max}) and Their Energies ($h\nu_{ICT}$) in Electronic Absorption Spectra, and Cyclic Voltammetry Data for Compounds 2d,e and 3b−e, Where Experiments Were Run in DMF unless Stated

		electron absorption spectra		CV (V *vs.* Ag/AgCl)			
compound	$\Sigma\sigma_p^{-}$ [26]	λ_{ICT}^{max} (nm)	$h\nu_{ICT}$ (eV)	$E_{ox}^{1/2}$	$E_{1red}^{1/2}$	$E_{2red}^{1/2}$	$E_{3red}^{1/2}$
2b	3.18	503	2.47	*a*	*a*	*a*	*a*
2d	4.45	565	2.20	+1.39[b]	−0.38	−0.64	−1.53[c]
				+1.41[b,d]	−0.57[d]	−0.69[d]	−1.39[c,d]
2e	5.04	589	2.11	+1.38[b]	−0.22	−0.43	−1.68[c]
3a	2.54	489	2.54	*a*	*a*	*a*	*a*
3b	3.18	513	2.42	+1.28[b]	−0.70	−0.82	
3c	3.81	530	2.34	+1.30[b]	−0.52	−0.72	−1.50[c]
3d	4.45	567	2.19	+1.32[b]	−0.36	−0.60	−1.41[c]
3e	5.04	588	2.11	+1.35[b]	−0.23	−0.45	−1.42[c]
poly(**2d**)	4.45	567	2.19	+1.20[e]	−0.54[e]	−0.71[e]	

[a] Sample too insoluble. [b] Irreversible peak. [c] Quasi-reversible peak. [d] Experiment run in DCM. [e] Experiment run in acetonitrile with the substrate as a film deposited on the working electrode.

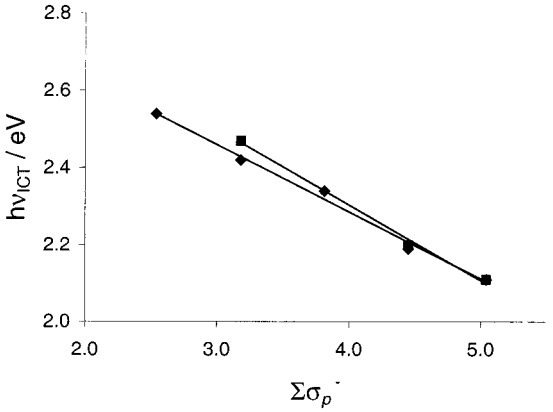

Figure 1. Absorption maxima (in eV) of compounds **2b**,**d**,**e** (■) and **3a**−**e** (◆) vs the sum of nucleophilic constants ($\Sigma\sigma_p^{-}$).

Table 2. Correlation of ICT Energies and Redox-potentials of Compounds 1, 2b,d,e, and 3a−e by eqs 1 and 2, Where All Values Are Taken from Measurements Carried out in DMF

eq 1	$h\nu_{ICT}^{0}$, eV	ρ^{-}, eV	r^a	n^b
1[ref 4]	3.10 ± 0.04	−0.18 ± 0.01	0.997	12
2b,**d**,**e**	3.09 ± 0.06	−0.20 ± 0.01	0.997	3
3a−**e**	2.98 ± 0.03	−0.17 ± 0.01	0.996	5

eq 2		$E_0^{1/2}$, V	ρ_{CV}^{-}, V	r	n
1[ref 4]	E_{ox}	+1.17 ± 0.08	0.10 ± 0.02	0.957	12
1[ref 4]	$E_{1red}^{1/2}$	−1.27 ± 0.08	0.20 ± 0.02	0.989	11
1[ref 4]	$E_{2red}^{1/2}$	−1.34 ± 0.04	0.17 ± 0.01	0.998	9
2[c]	$E_{1red}^{1/2}$	−1.6	0.27		2
2[c]	$E_{2red}^{1/2}$	−2.2	0.35		2
3a−**e**	E_{ox}	+1.16 ± 0.01	0.04 ± 0.003	0.985	4
3a−**e**	$E_{1red}^{1/2}$	−1.49 ± 0.04	0.25 ± 0.01	0.997	4
3a−**e**	$E_{2red}^{1/2}$	−1.46 ± 0.06	0.20 ± 0.01	0.989	4

[a] Correlation coefficient. [b] Number of compounds in series. [c] Estimated by two points.

terthiophenedithiino moieties. The electron-accepting ability of the fluorene compounds varies between derivatives, such that **3b** exhibits two single-electron reversible reduction processes ($E_{1red}^{1/2}$ and $E_{2red}^{1/2}$), while **2d**,**e** and **3c**−**e** deliver a third, additional single-electron quasi-reversible reductive wave between −1.41 and −1.53 V ($E_{3red}^{1/2}$). For instance, in Figure 2, the three reversible electron processes correspond to the formation of $\mathbf{3d}^{-\bullet}$ (−0.36 V), $\mathbf{3d}^{2-}$ (−0.60 V), and $\mathbf{3d}^{3-\bullet}$ (−1.41 V).

In fashion similar to the electronic absorption data, we can relate the electroactivity of the fluorene derivatives to the electron-withdrawing ability of the substituents in the fluorene ring. Thus, by using eq 2, we can determine the substituent sensitivity for compounds

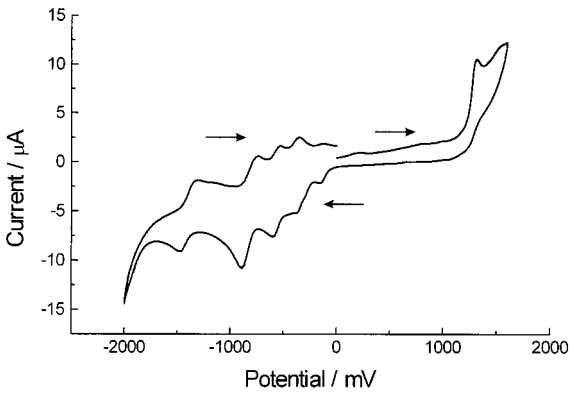

Figure 2. Cyclic voltammogram of **3d** (ca. 10^{-3} M) in DMF solution, containing 0.1 M $Bu_4N^+PF_6^-$, Au working electrode, Ag/AgCl reference electrode, scan rate 100 mVs^{-1}.

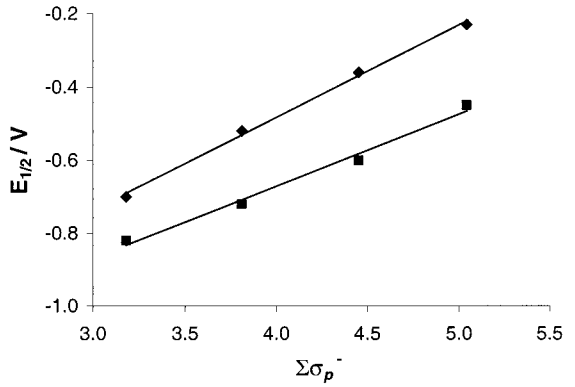

Figure 3. Plot of $E_{1red}^{1/2}$ (◆) and $E_{2red}^{1/2}$ (■) for compounds **3b**−**e** vs the sum of nucleophilic constants ($\Sigma\sigma_p^{-}$).

2b,**d**,**e** and **3a**−**e** toward the individual redox processes (i.e., E_{ox}, $E_{1red}^{1/2}$, $E_{2red}^{1/2}$ and $E_{3red}^{1/2}$).

$$E^{1/2} = E_0^{1/2} + \rho_{CV}^{-}\Sigma\sigma_p^{-} \qquad (2)$$

The values for $E_0^{1/2}$ and ρ^{-}_{CV} (sensitivity parameter) for series **1** and **3** are collated in Table 2 (for series **2**, an approximate estimation was made by two points; this is a mere indication that the values are of the same order of magnitude, rather than providing accurate quantitative characteristics). In each case, the third reduction process fails to show any relationship with the substituents on the fluorene ring (Table 1), while $E_{1red}^{1/2}$ and $E_{2red}^{1/2}$ give good linear trends ($r > 0.98$), (Figure 3). Although E_{ox} also shows some correlation with $\Sigma\sigma_p^{-}$, the effect of the electron-withdrawing groups

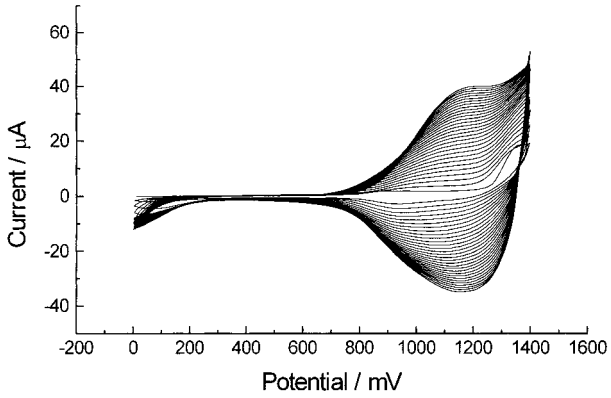

Figure 4. Electropolymerization of terthiophene **2d** (0.01 M) in DCM, containing 0.1 M $Bu_4N^+PF_6^-$, using successive scans at 200 mV s^{-1}, Au working electrode and Ag/AgCl reference electrode.

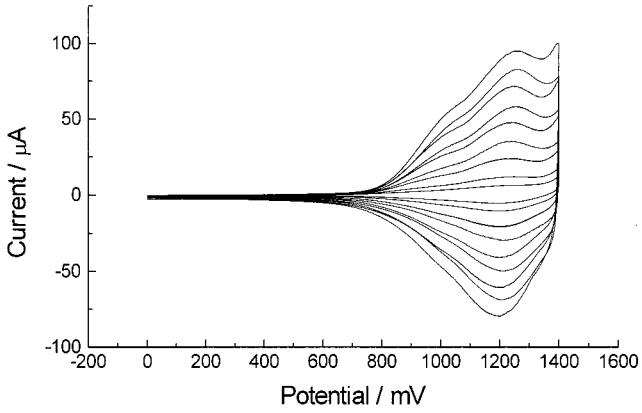

Figure 5. Cyclic voltammograms of poly(**2d**) in monomer-free acetonitrile solution, containing 0.1 M $Bu_4N^+PF_6^-$ at varying scan rates: 25 (inner cycle), 50, 100, 150, 200, 250, 300, 350, and 400 (outer cycle) mV s^{-1}.

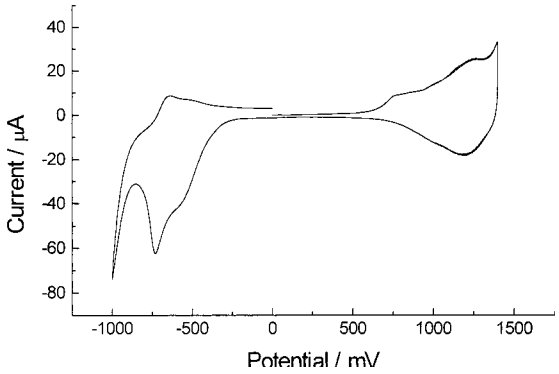

Figure 6. Cyclic voltammogram of poly(**2d**) in monomer-free acetonitrile solution, containing 0.1 M $Bu_4N^+PF_6^-$: scan rate 200 mV s^{-1}. Electrochemical band gap ca. 1.0 V.

upon the donor unit in compounds **3b**−**e** is very weak ($\rho_{CV}^- = 0.04$ V) and even weaker than in **1** ($\rho_{CV}^- = 0.10$ V). The additional 1,4-dithiino spacer in **3** (as compared to the series **1**), decreases the electronic effects of the fluorene moiety, thereby weakening the influence of the acceptor unit upon the oxidative ability of the thiophene fragment. This feature is actually to our advantage, since the preparation of stronger electron acceptors of the fluorene series will not give rise to thiophene units possessing unfavorably high oxidation potentials, which would render the polymerization of these derivatives by chemical/electrochemical oxidation either difficult or impossible.[27] On the other hand, the properties of the resulting polymers (from the viewpoint of ICT onto the fluorene ring) can be widely tuned by variation of the substituents within the fluorene moiety.

The values of ρ^-_{CV} for series **3** were 0.25 ($E_{1red}^{1/2}$) and 0.20 ($E_{2red}^{1/2}$), which are slightly higher than the values for series **1** (0.20 and 0.17 V, respectively). Although, we were not able to do a similar study for series **2**, we anticipate that the electron-accepting properties will be closely related to those of **3b**−**3e**. Indeed, the values of $E_{1red}^{1/2}$ and $E_{2red}^{1/2}$ for compounds **2d** and **3d** are very similar (Table 1).

Polymerization of Compound 2d. Poly(**2d**) was obtained by the electrochemical oxidation of **2d** in DCM solution (substrate ca. 10^{-2} M, $nBu_4N^+PF_6^-$ 0.1 M, gold working electrode, platinum wire counter electrode, Ag/AgCl reference electrode, 20 °C), using successive scans ranging from 0 to 1.40 V with a scan rate of 200 mV/s. Under these conditions, a dark blue film deposited on the surface of the gold electrode; Figure 4 shows the typical polymer growth over 30 cycles. Figure 5 represents the response of poly(**2d**), in acetonitrile monomer-free solution, to p-doping up to +1.40 V at varying scan rates between 25 and 400 mV/s. The relationship between the maximum peak current and the scan rate is linear (correlation coefficient $r > 0.999$); this behavior is indicative of a redox-active polymer attached to the electrode surface and also demonstrates the stability of the polymer toward p-doping.

The cyclic voltammogram of a thin film of poly(**2d**) in acetonitrile is shown in Figure 6. A small anodic irreversible peak at +0.76 V is followed by a reversible oxidation process (observed at +1.20 V). While the main oxidation peak for the donor poly(thiophene) component (+1.20 V) is lower than the corresponding oligothiophene unit in **2d** (ca. +1.41 V in DCM, Table 1), the electron-accepting properties of the fluorene moiety are mostly retained in the polymer. Thus, the first two reduction waves, $E_{1red}^{1/2} = -0.54$ V and $E_{2red}^{1/2} = -0.71$ V, for poly(**2d**) are very similar to those of **2d** (−0.57 and −0.69 V in DCM and −0.38 and −0.64 V in DMF, respectively); however, the reduction peaks in the polymer appear to be quasi-irreversible. Beyond the limits of the CV shown in Figure 6 (>+1.40 V and <−1.00 V), the polymer decomposed. Consequently, we are not able to comment on the third reduction process for poly(**2d**), which is clearly seen in the monomer.

Poly(**2d**) was also prepared by chemical oxidation with anhydrous $FeCl_3$ using nitrobenzene as the solvent. Unfortunately, we were not able to deduce the molecular weight of the polymer due to its poor solubility, however, elemental analysis showed that the chemically prepared polymer was efficiently cleaned after Soxhlet extraction with methanol. The UV−visible spectrum of the chemically prepared material (Figure 7) is almost identical to that obtained after electrochemical polymerization. A direct comparison with the spectrum obtained from the monomer (**2d**, Figure 7), shows that the ICT band in the polymer is nicely preserved (λ_{ICT} for poly(**2d**) is 567 nm). A shoulder at 620 nm is seen in the spectrum of poly(**2d**), arising from an increase in conjugation within the polythiophene chain; the corresponding absorption maximum for the terthiophene unit in **2d** is observed at 439 nm. The longest wavelength absorption edge of poly(**2d**) indicates an optical band gap of 1.7 eV, which is far greater than the band gap determined electrochemically (1.0 V, measured as the difference between the onset potentials for p- and n-doping; Figure

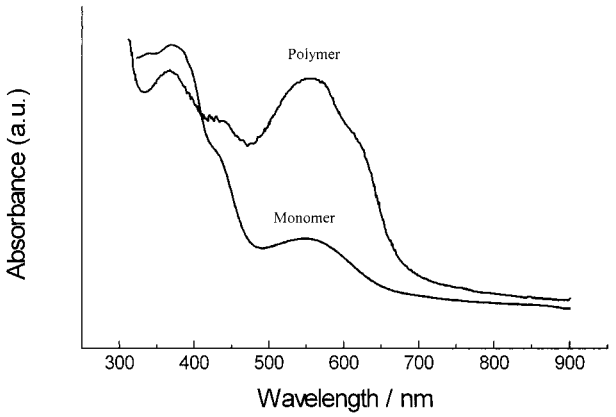

Figure 7. Absorption spectra of **2d** and chemically prepared poly(**2d**) in DMF solution.

6). This large discrepancy in band gap values tends to suggest that the electroactivity of the fluorene unit is substantially independent of the polythiophene chain; i.e., p-doping (≈+0.7 V) occurs in the polythiophene main chain whereas n-doping (≈−0.3 V) takes place on the fluorene site of the polymer and is expected to be more localized.

FTIR Spectroscopy. In Situ Spectroelectrochemistry and Photoinduced Absorption. Molecules with extended π-electron delocalization are characterized by strong coupling between vibrational and electronic effects due to a large electron−phonon coupling. Thus, vibrational spectroscopy on CPs gives an insight into their electronic properties. In particular, the IR spectra of CPs in their oxidized (reduced) or photoexcited, conductive forms are characterized by absorption changes due to the modification of the polymer band structure[28,29] and by strong new IR bands due to the activation of infrared active vibration (IRAV) bands.[30,31] The characteristics of these latter spectral features are strongly related to the effective conjugation length of the macromolecule and to the delocalization of the radical ions (the so-called polarons) and/or to charged photoexcited states formed on the polymer by the redox process or by illumination.

The evolution of the IR spectrum of poly(**2d**) during its electrochemical oxidation is depicted in Figure 8. The broad and intense band in the high-frequency part of the spectrum (5000−2000 cm^{-1} in Figure 8a) is related to the low energy, intragap electronic transitions of the radical cations formed by oxidation. The IRAV range, which is shown in detail in Figure 8b, is characterized by rather broad bands and an ill-defined pattern. According to the terthiophene nature of the repeating unit, the spectrum shows similarity with that of electrochemically oxidized polythiophene.[32] Apart from small changes in frequencies and relative intensities, as the polymer is increasingly oxidized (ca. +0.48 to +1.2 V), three main bands emerge at about 1380, 1190, and 1055 cm^{-1}. These bands show high correspondence to the three main IRAV modes reported for thiophene-based CPs.[30b,32] The broadness of the IRAV bands of poly(**2d**) in its oxidized form is suggesting a rather high level of delocalization for the radical cations.[30] Note that the sharp peak at 843 cm^{-1} is due to the incorporation of PF_6^- counterions, which balance the positive charge formed on the polymer by electrochemical oxidation.

The photoinduced IR spectrum of poly(**2d**) is shown in Figure 9. The observance of two electronic bands,

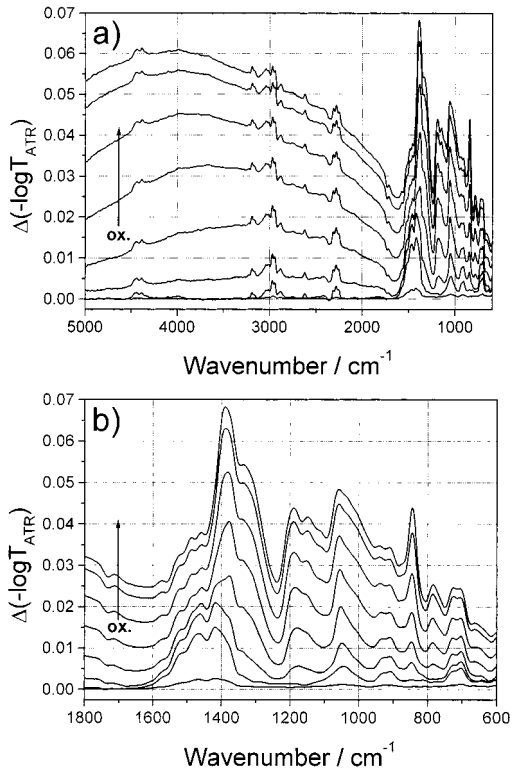

Figure 8. In situ FTIR difference spectra during electrochemical oxidation of poly(**2d**). Sequence: bottom ($E \approx 0.48$ V vs Ag/AgCl wire) to top ($E \approx 1.2$ V vs Ag/AgCl wire). Key: (a) extended range; (b) IRAV range.

with maxima at about 3700 cm^{-1} and above 7000 cm^{-1}, out of the detection range (Figure 9a), as well as of new vibrational bands in the IRAV vibrational regime (Figure 9b), clearly indicate the charged nature of long-living photoexcitations.[30,33] Again, three intense bands are detected, at about 1340, 1150, and 1050 cm^{-1}. Sharp, downward pointing spectral features around 1500 cm^{-1} and near the maxima of the IRAV bands, around 1340 and 1150 cm^{-1}, are due to the bleaching of the bands seen in the poly(**2d**) IR absorption spectrum, also shown in Figure 9. Interestingly, the two bands at high-frequency maintain a quite broad shape while the band at ca. 1050 cm^{-1} exhibits a narrow shape. Moreover, the first two bands shift, with respect to those in the oxidized polymer spectrum, toward lower frequency, whereas the third one remains at almost the same wavenumber. The absence of electrolyte counterions, which may introduce a "pinning" effect in the electrochemically oxidized material,[31b] explains a more delocalized nature for charged states in the photoexcited sample and, therefore, the softening observed for the bands at 1340 and 1150 cm^{-1}.[30b,34] On the other hand, the sharpening of the band at 1050 cm^{-1} in the photoinduced IR spectrum, together with its lack of frequency shift, indicate that this IRAV band is not affected like the other two. Since long-living and negatively charged states in poly(**2d**) should be mainly confined within the electron-accepting fluorene moiety, a localized negative charge can occur also in the photoexcited polymer.

Conclusions

We have prepared a series of thiophene systems bearing a range of substituted 1,3-dithiole-2-ylidene-fluorene units as strong electron acceptor species. These materials (**2b**,**d**,**e** and **3a**−**e**) exhibit a strong correlation

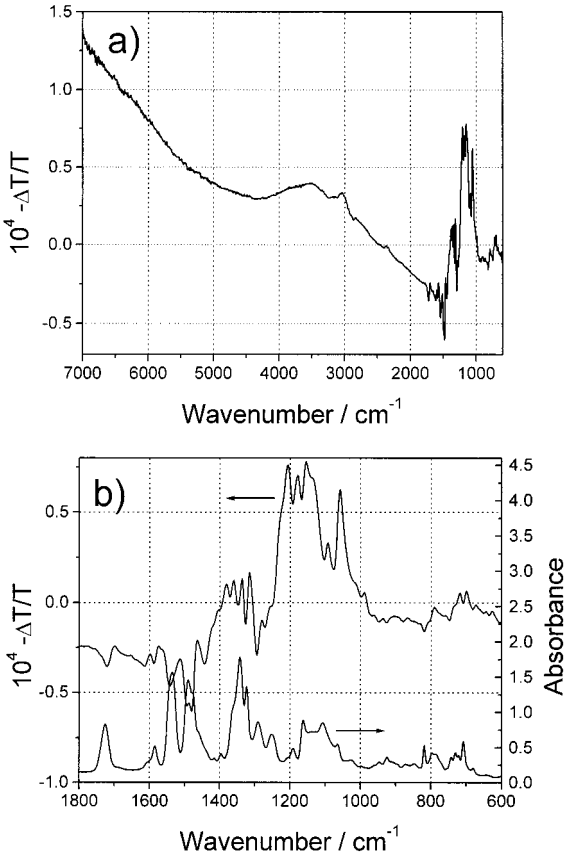

Figure 9. Photoinduced FTIR absorption of poly(**2d**); excitation at $\lambda = 488$ nm, 30 mW cm^{-2}. Key: (a) full range; (b) IRAV range (upper plot), compared to the IR absorption of the neutral polymer (lower plot).

between ICT and the sum of the nucleophilic constants ($\sum\sigma_p^-$) of the fluorene substituents. Similarly, the first two reduction processes for series **3** are also highly influenced by $\sum\sigma_p^-$, whereas the oxidation process is only slightly influenced by the fluorene structure.

Polymerization of **2d** has been achieved electrochemically and by oxidation with ferric (III) chloride. The difference in λ_{ICT}^{max} (using DMF as the solvent), for the analogous series **2d**, **3d** and poly(**2d**) is negligible (2.20, 2.19, and 2.19 eV, respectively). This shows that the degree of intramolecular charge-transfer can be finely tuned in polymeric systems as well as in molecular species by the variation of substituents on the fluorene ring. In this context, we provide some evidence toward the design of fluorene-based polythiophenes of the type poly(**2d**) which give photoexcited states at predicted wavelengths.

The values for $E_{1red}^{1/2}$ and $E_{2red}^{1/2}$ (Table 1) for compounds **2d** and **3d** are similar. The corresponding redox processes for poly(**2d**) are difficult to compare with the molecular systems, since the CV of poly(**2d**) in DMF was ill-defined. Nevertheless, the general reductive behavior of poly(**2d**) is commensurate with that of **2d** and **3d**; a more detailed electrochemical study on a series of fluorene-containing polythiophenes (based on poly(**2d**)) would be extremely worthwhile.

The photoinduced infrared spectrum of poly(**2d**) provides evidence of long-lived charged-separated states in the polymer. Furthermore, the broad IRAV bands are indicative of highly delocalized radical cations, suggesting that the electron donating site of the polymer is situated within the polythiophene backbone. Conversely, the electron-accepting site is proposed to be localized within the fluorene unit. The above criteria are essential for the development of fluorene-containing polythiophenes as useful alternatives to PPV−C_{60} composites in plastic photovoltaic cells. The ability to control the donor−acceptor interaction by means of precise structural design is certainly a major advantage over fullerene-based systems.

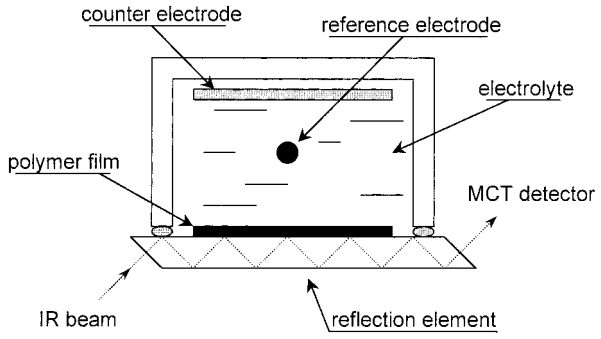

Figure 10. Cell for in situ ATR infrared spectroelectrochemistry.

Experimental Section

Instrumentation. Melting points were taken using an Electrothermal melting point apparatus and are uncorrected. ^{1}H NMR spectra were recorded on a Bruker AC 250 instrument; chemical shifts, given in ppm, are relative to tetramethylsilane as internal standard; all *J* values are in Hz. IR spectra were recorded on a Mattson Genesis Series FTIR spectrometer. High-resolution mass spectra (HRMS) were recorded on a 7070E VG Analytical mass spectrometer.

Reagents and Solvents. Fluorene **6a** and DMAD were purchased from Aldrich. Anhydrous DCM, DMF, and acetonitrile used in CV experiments (Aldrich), as well as $nBu_4N^+PF_6^-$ (Fluka), were electrochemical grade purity and used as received. The following compounds were obtained as described elsewhere: **6b**,**d**,[16,17] **6c**,**e**,[4] **7**,[19] **8**,[23] and **13**.[25]

Electrochemistry. The measurements were performed on a BAS CV50W voltammetric analyzer with *iR* compensation, using anhydrous DCM, acetonitrile or DMF as the solvents, Ag/AgCl as the reference electrode and platinum wire and gold disk (2.0 mm diameter) as the counter and working electrodes, respectively. All solutions were degassed (N_2) and contained the substrate in concentrations ca. 10^{-3} M, together with $nBu_4N^+PF_6^-$ (0.1 M) as the supporting electrolyte. The electropolymerization experiment was conducted in DCM and all polymer films were studied in acetonitrile solution containing $nBu_4N^+PF_6^-$ (0.1 M) as the supporting electrolyte. All experiments were carried out at room temperature.

Fourier Transform Infrared Spectroscopy. In situ attenuated total reflection FTIR spectroelectrochemistry has been performed using the cell shown in Figure 10. Details on the technique and the setup are given elsewhere.[35] For the present work poly(**2d**) was drop-cast from solution in dry DMF on a Ge reflection element, which acts as a waveguide for the infrared beam and as the working electrode. A Pt foil and a Ag/AgCl wire electrode were used as counter and reference electrodes, respectively. Infrared spectra were recorded consecutively during a potential sweep at a rate of 5 mV s^{-1}, using 0.1 M $nBu_4N^+PF_6^-$ in dry CH_3CN as supporting electrolyte. Specific spectral changes during the electrochemical oxidation were obtained by relating subsequent spectra to the spectrum at 0.4 V, which was chosen as the reference. Each spectrum, calculated as $\Delta(-\log T_{ATR})$, where T_{ATR} is the transmission in the ATR geometry, covers a range of about 90 mV in the cyclic voltammogram. Experiments were made at room temperature and under argon. For photoinduced FTIR absorption, a drop-cast film of poly(**2d**) on KBr pellet was placed in a liquid N_2 bath cryostat with ZnSe windows. The sample was illuminated

in 45° geometry by the 488 nm line of an Ar^+ laser, with an intensity of 30 mW cm^{-2}. The photoinduced changes in the infrared absorption spectrum were measured by collecting 300 repetitions of 10 co-added single beam spectra taken under illumination and of 10 co-added single beam spectra taken in the dark. Combining the respective spectra the photoinduced absorption was calculated as $-\Delta T/T$. During measurements, the vacuum was better than 10^{-5} mbar. FTIR spectra were recorded with a resolution of 4 cm^{-1}, using a Bruker IFS 66S spectrometer equipped with a liquid N_2 cooled MCT detector.

6-Diethoxymethyl-1,3-dithiolo[4,5-*b*]1,4-dithiine-2-thione-5-carboxaldehyde (9). A mixture of **7** (3.46 g, 18 mmol), **8** (2.68 g,17.2 mmol), toluene (50 mL), and 2,6-lutidine (0.5 mL) was stirred at 70 °C over 45 min, cooled to room temperature, and filtered through a 3 cm layer of silica. The silica was washed with toluene (50 mL), and the volume of filtrate was reduced in vacuo to ca. 25 mL. After the filtrate was cooled to 0 °C, the crude product was isolated by filtration, and the filtrate was evaporated in vacuo to dryness. The crude product was treated with charcoal (1 g) in ethanol (150 mL) under reflux; the charcoal was filtered off and washed with hot ethanol (50 mL). After the volume of the ethanolic solution was reduced to 50 mL, the pure product was obtained as yellow needles. The mother liquor was added to the residue from the evaporation of the toluene mother liquor, and the mixture was treated three times with portions of charcoal (0.5 g each) under reflux. After the volume of the solution was reduced to ca. 25 mL, the second crop of pure product was obtained. Overall yield 2.85 g (48%); mp 111−114 °C (lit. 103 °C).[24] ^{1}H NMR ($CDCl_3$): δ/ppm 10.05 (s, 1H), 5.68 (s, 1H), 3.69 (m, 4H), 1.28 (t, *J* 7.1, 6H). HRMS: calcd for $C_{11}H_{12}O_3S_5$, 351.93900; found, 351.93960.

5-Hydroxymethyl-6-diethoxymethyl-1,3-dithiolo[4,5-*b*]1,4-dithiine-2 thione (10). $NaBH_4$ (1.5 g, 39 mmol) was added to a stirred solution of aldehyde **9** (1.64 g, 4.66 mmol) in THF (50 mL) at 20 °C. After 2 min, the reaction mixture was poured into saturated aqueous $NaHCO_3$ (100 mL); KBr (10 g) was added, and the product was extracted with ethyl acetate. The extract was dried over $MgSO_4$ and evaporated in vacuo to dryness, affording 1.61 g (98%) of the product as a yellow-brown solid, mp 101−106 °C, which was used in the next step without further purification. An analytical sample (from hexane−ethyl acetate) was obtained as a yellow crystalline solid, mp 108−109 °C. ^{1}H NMR ($CDCl_3$): δ/ppm 5.33 (s, 1H), 4.47 (d, 2H, *J* 6.6), 3.62 (4H, m), 2.44 (1H, t, *J* 6.6), 1.26 (6H, t, *J* 7.2). IR (KBr): ν_{max}/cm^{-1} 3461, 2973, 2875, 1157, 1100, 1063, 902, and 506. EIMS (M^+ − EtOH): 308.

5-Bromomethyl-6-diethoxymethyl-1,3-dithiolo[4,5-*b*]1,4-dithiine-2-thione (11). Carbon tetrabromide (1.16 g, 3.48 mmol) and triphenylphosphine (0.570 g, 2.18 mmol) were added to a solution of **10** (0.539 g, 1.74 mmol) and 2,6-lutidine (4.8 mmol) in dry THF (10 mL) under dry nitrogen, and the mixture was stirred over 40 min at 20 °C. The solvent was removed in vacuo and the residue was subjected to flash chromatography (silica, DCM:petroleum ether 1:1) to give 0.427 g (63%) of **11** as a yellow crystalline solid, mp 102−104 °C. ^{1}H NMR ($CDCl_3$): δ/ppm 5.28 (s, 1H), 4.39 (s, 2H), 3.62 (m, 4H), 1.27 (6H, t, *J* 7.2). IR (KBr): ν_{max}/cm^{-1} 2976, 2900, 1321, 1209, 1141, 1075, and 561. HRMS: calcd for $C_{11}H_{13}{}^{79}BrO_2S_5$, 415.87024; found, 415.87308.

Thienodithiino[3,4-*b*:5,6-*e*]1,3-dithiole-2-thione (4). $Na_2S\cdot 9H_2O$ (2.5 g, 10 mmol) and methanol (75 mL) were placed in a column equipped with a porous glass plate at the bottom inlet, and the mixture was saturated with hydrogen sulfide [obtained by treating a mixture of sodium sulfide (20 g, 80 mmol) and water (20 mL) with concentrated HCl (18 mL)], by bubbling the gas through the base of the column. The solution was cooled to −20 °C and was added, in one portion on stirring, to a chilled solution (−20 °C) of **11** (0.383 g, 1.0 mmol) in THF (25 mL). After 2.5 min, concentrated aqueous HCl (7 mL) was added, and the mixture was warmed to 50 °C and filtered. The volume of the filtrate was reduced in vacuo to ca. 20 mL, water (20 mL) was added, and the precipitate was filtered and washed with water. A solution of the crude product in a mixture of THF (30 mL) and ethanol (70 mL) was treated with charcoal (0.5 g) under reflux, filtered, and evaporated in vacuo to a volume of ca. 15 mL. Water (5 mL) was added, and the product was filtered to give 0.105 g (34%) of **4** as a yellow solid, mp 201−206 °C dec. ^{1}H NMR ($CDCl_3$): δ/ppm 7.21 (s). IR (KBr): ν_{max}/cm^{-1} 3094, 3071, 1477, 1331, 1069, 792, and 513. HRMS: calcd for $C_7H_2S_6$, 277.84808; found, 277.84844.

2-Methylthiothienodithiino[3,4-*b*:5,6-*e*]1,3-dithiolium triflate (5). A mixture of **4** (0.100 g, 0.36 mmol), dry DCM (2 mL), and methyl trifluoromethanesulfonate (0.16 mL, 1.4 mmol) was stirred at 20 °C over 16 h. Dry diethyl ether (10 mL) was added, and the precipitate was washed with a further amount of diethyl ether and dried at room temperature under dry nitrogen, affording the product as an orange-brown solid (crystallosolvate **5**·CH_2Cl_2, 0.110 g, 53%). ^{1}H NMR (acetone-d_6): δ/ppm 7.79 (2H, s), 5.61 (2H, s, CH_2Cl_2), 3.33 (3H, s). IR (KBr): ν_{max}/cm^{-1} 3087, 1451, 1268, 1253, 1157, 1028, 810, and 637.

General Procedure for 9-(Thienodithiino[3,4-*b*:5,6-*e*-1,3-dithiole-2-ylidene) Polynitrofluorene Derivatives (3a−e). To a mixture of salt **5** and the corresponding fluorene derivative **6** (in a 1:1 molar ratio), was added pyridine or DMF (dry pyridine for dinitro derivatives or DMF for trinitrofluorenes, 0.25 mL per 50 mg of the solid mixture), and the reaction mixture was stirred at the desired temperature (60 °C for **6e**, 90 °C for others) for 30 min under dry nitrogen. Ethanol (2 mL) was added and the precipitate was filtered and recrystallized from a suitable solvent (DMF for **3a** and **3c** or DMF:ethanol for others).

9-(Thienodithiino[3,4-c:5,6-d]-1,3-dithiole-2-ylidene)-2,7-dinitrofluorene (3a). Yield 25%, mp >250 °C. ^{1}H NMR (DMSO-d_6, 100 °C): δ/ppm 8.61 (2H, d, 1.7), 8.40 (2H, d, *J* 8.4), 8.29 (2H, dd, *J* 8.4 and 1.9), 7.73 (2H, s); IR (KBr): ν_{max}/cm^{-1} 3101, 1516, 1493, 1336, 828, and 728. HRMS: calcd for $C_{20}H_8N_2O_4S_5$, 499.90875; found, 499.90861.

9-(Thienodithiino[3,4-c:5,6-d]-1,3-dithiole-2-ylidene)-2,7-dinitrofluorene-4-carboxylic Acid (Triethylene Glycol Monoethyl Ether) Ester (3b). Yield 35%, mp > 250 °C. ^{1}H NMR (DMSO-d_6, 100 °C): δ/ppm 8.70 (1H, d, *J* 2.0), 8.57 (1H, d, *J* 2.0), 8.54 (1H, d, *J* 8.8), 8.48 (1H, d, *J* 2.0), 8.19 (1H, dd, *J* 8.8 and 2.0), 7.72 (2H, s), 4.66 (2H,m), 3.90 (2H, m), 3.71−3.40 (10H, m), 1.07 (3H, t, *J* 7.0). IR (KBr): ν_{max}/cm^{-1} 3095, 2865, 1727, 1524, 1491, 1330, 1165, 1103, and 826.

9-(Thienodithiino[3,4-c:5,6-d]-1,3-dithiole-2-ylidene)-2,4,7-trinitrofluorene (3c). Yield 40%, mp >250 °C. ^{1}H NMR (DMSO-d_6, 100 °C): δ/ppm 8.88 (1H, d, *J* 1.6), 8.69 and 8.68 (2H, overlapping singlets), 8.27 (1H, dd, *J* 8.7 and 1.5), 8.17 (1H, d, *J* 8.7) and 7.75 (2H, s). IR (KBr): ν_{max}/cm^{-1} 3089, 1525, 1479, 1406, 1339, 1226, and 827. HRMS: calcd for $C_{20}H_7N_3O_6S_5$, 544.89386; found, 544.89544.

9-(Thienodithiino[3,4-d:5,6-c]-1,3-dithiole-2-ylidene)-2,5,7-trinitrofluorene-4-carboxylic Acid (Triethylene Glycol Monomethyl Ether) Ester (3d). Yield 70%, mp >250 °C. ^{1}H NMR (DMSO-d_6, 100 °C): δ/ppm 9.01 (1H, d, *J* 1.7), 8.93 (1H, d, *J* 1.7), 8.66 (1H, d, *J* 1.7), 8.51 (1H, d, *J* 1.7), 7.76 (2H, s), 4.44 (2H, t, *J* 5.0), 3.82 (2H, t, *J* 5.0), 3.63−3.51 (6H, m), 3.43 (2H, m), 3.25 (3H, s). IR (KBr): ν_{max}/cm^{-1} 3091, 2870, 1720, 1528, 1476, 1333, 1158, 1101, and 707. HRMS: calcd for $C_{28}H_{21}S_5O_{11}N_3$, 734.97797; found, 734.975 88.

9-(Thieno[3,4-d]-1,3-dithiole-2-ylidene)-2,4,5,7-tetranitrofluorene (3e). Yield 78% of crystallosolvate **3e**·DMF, stable at 110 °C/2 mm; mp > 250 °C. ^{1}H NMR (DMSO-d_6, 100 °C): δ/ppm 9.10 (2H, s, br), 8.69 (2H, s, br), 7.98 (1H, s, DMF), 7.76 (2H, s), 2.87 and 2.78 (DMF, shoulders on water peak at 2.83 ppm). IR (KBr): ν_{max}/cm^{-1} 3098, 2922 (DMF), 1663 (DMF), 1543, 1461, 1335, 1249, 1162, and 817. Anal. Calcd for $C_{23}H_{13}N_5O_9S_5$ (**3e**·DMF): C, 41.62; H, 1.97; N, 10.55. Found: C, 41.25; H, 1.90; N, 9.91.

General Procedure for 9-[2,8-Di(2-thienyl)thienodithiino[3,4-*b*:5,6-*e*-1,3-dithiole-2-ylidene]polynitrofluorene Derivatives (2b,d,e). Methyl triflate (0.1 mL, 0.9 mmol) was added to a suspension of **13** (0.044 g, 0.10 mmol) in dry DCM (0.5 mL) under dry nitrogen and the mixture was stirred for 3 d at room temperature. Dry diethyl ether (1.5 mL) was added on stirring, the solution was decanted from the precipitate, and the residue was washed with two portions of dry diethyl

ether under dry nitrogen. The corresponding fluorene derivative **6** (0.1 mmol) and the solvent (0.5 mL, dry pyridine for dinitrofluorenes or dry DMF for others) were added to the residue and the mixture was stirred under nitrogen for 30 min at 80−90 °C. After cooling, the mixture was diluted with ethanol (1.5 mL), and the precipitate was filtered, washed with water and ethanol, and recrystallized from an appropriate solvent (DMF for **2b**,**e** or dioxane for **2d**).

9-[2,8-Di(2-thienyl)thienodithiino[3,4-*b*:5,6-*e*-1,3-dithiole-2-ylidene]-2,7-dinitrofluorene-4-carboxylic Acid (Triethylene Glycol Monoethyl Ether) Ester (2b). Yield 40%, mp >250 °C. ^{1}H NMR (DMSO-d_6, 110 °C): δ/ppm 8.82 (1H, d, *J* 1.9), 8.68 (1H, d, *J* 2.0), 8.59 (1H, d, *J* 8.8), 8.52 (1H, d, *J* 1.9), 8.26 (1H, dd, *J* 8.8 and 1.9), 7.75 (2H, dd, *J* 5.2 and 1.0), 7.48 (2H, dd, *J* 3.6 and 1.0), 7.25 (2H, dd, *J* 5.2 and 3.6), 4.67 (2H,m), 3.89 (2H, m), 3.70−3.30 (10H, m), 1.07 (3H, t, *J* 6.8). (KBr): ν_{max}/cm^{-1} 33082, 2864, 1725, 1524, 1497, 1344, 1022, and 681.

9-[2,8-Di(2-thienyl)thienodithiino[3,4-*b*:5,6-*e*-1,3-dithiole-2-ylidene]-2,4,7-trinitrofluorene-5-carboxylic Acid (Triethylene Glycol Monomethyl Ether) Ester (2d). Yield 44%, mp > 250 °C. ^{1}H NMR (DMSO-d_6, 110 °C): δ/ppm 8.98 (1H, s), 8.90 (1H, s), 8.64 (1H, s), 8.50 (1H, s), 7.75 (2H, dd, *J* 5.2 and 1.0), 7.46 (2H, dd, *J* 3.6 and 1.0), 7.24 (2H, dd, *J* 5.2 and 3.6), 4.43 (2H, m), 3.81 (2H, m), 3.62−3.50 (6H, m), 3.43 (2H, m), 3.25 (3H, s). IR (KBr): ν_{max}/cm^{-1} 3093, 2864, 1722, 1530, 1480, 1339, 1101, and 703. Anal. Calcd for $C_{36}H_{25}N_3O_{11}S_7$: C, 48.04; H, 2.80; N, 4.67. Found: C, 47.68; H, 2.92; N, 4.50.

9-[2,8-Di(2-thienyl)thienodithiino[3,4-*b*:5,6-*e*-1,3-dithiole-2-ylidene]-2,4,5,7- tetranitrofluorene (2e). Yield 50%, mp > 250 °C. ^{1}H NMR (DMSO-d_6, 110 °C): δ/ppm 9.09 (2H, d, *J* 1.6), 8.70 (2H, d, *J* 1.7), 7.76 (2H, dd, *J* 5.2 and 1.0), 7.49 (2H, dd, *J* 3.7 and 1.0), 7.25 (2H, dd, *J* 5.2 and 3.6). IR (KBr): ν_{max}/cm^{-1} 3092, 1542, 1482, 1357, 1338, 1317, and 706.

Poly{9-[2,8-Di(2-thienyl)thienodithiino[3,4-*b*:5,6-*e*-1,3-dithiole-2-ylidene]-2,4,7-trinitrofluorene-5-carboxylic Acid (Triethylene Glycol Monomethyl Ether) Ester} [Poly-(2d)]. To a solution of **2d** (0.131 g, 0.15 mmol) in nitrobenzene (30 mL) at 60 °C was added anhydrous iron(III) chloride (0.200 g, 1.23 mmol). After the reaction mixture was stirred at 60 °C for 20 h, the volume of the solvent was reduced to ca. 15 mL under vacuum. Methanol (50 mL) was added, and the precipitate was washed with methanol and ether to give poly(**2d**) as a black-violet solid (0.110 g, 84% yield). Anal. Calcd for $C_{36}H_{23}N_3O_{11}S_7$: C, 48.16; H, 2.56; N, 4.68. Found: C, 47.41; H, 2.40; N, 3.81.

Acknowledgment. We thank The Royal Society and NATO for a Postdoctoral Fellowship (to I.M.S.). The work in Linz was performed within the Christian Doppler Society's dedicated laboratory for Plastic Solar Cells.

References and Notes

(1) Part 11 of the series "Electron Acceptors of the Fluorene Series". For part 10 (and references on previous parts), see: Perepichka, I. F.; Popov, A. F.; Orekhova, T. V.; Bryce, M. R.; Andrievskii, A. M.; Batsanov, A. S.; Howard, J. A. K.; Sokolov, N. I. *J. Org. Chem.* **2000**, *65*, 3053.

(2) Goldberg, I. *Acta Crystallogr. B* **1973**, *29*, 440.

(3) Perepichka, I. F.; Kuz'mina, L. G.; Perepichka, D. F.; Bryce, M. R.; Goldenberg, L. M.; Popov, A. F.; Howard, J. A. K. *J. Org. Chem.* **1998**, *63*, 6484.

(4) Skabara, P. J.; Serebryakov, I. M.; Perepichka, I. F. *J. Chem. Soc., Perkin Trans. 2* **1999**, 505.

(5) (a) Perepichka, I. F.; Popov, A. F.; Orekhova, T. V.; Bryce, M. R.; Vdovichenko, A. N.; Batsanov, A. S.; Goldenberg, L. M.; Howard, J. A. K.; Sokolov, N. I.; Megson, J. L. *J. Chem. Soc., Perkin Trans. 2* **1996**, 2453. (b) Perepichka, I. F.; Perepichka, D. F.; Bryce, M. R.; Goldenberg, L. M.; Kuz'mina, L. G.; Popov, A. F.; Chesney, A.; Moore, A. J.; Howard, J. A. K.; Sokolov, N. I. *Chem. Commun.* **1998**, 819.

(6) Semenenko, N. M.; Abramov, V. N.; Kravchenko, N. V.; Trushina, V. S.; Buyanovskaya, P. G.; Kashina, V. L.; Mashkevich, I. V. *Zh. Org. Khim.* **1985**, *55*, 324 (in Russian).

(7) (a) Perepichka, I. F.; Perepichka, D. F.; Bryce, M. R.; Chesney, A.; Popov, A. F.; Khodorkovsky, V.; Meshulam, G.; Kotler, Z. *Synth. Met.* **1999**, *102*, 1158. (b) Perepcihka, D. F.; Perepichka, I. F.; Bryce, M. R.; Moore, A. J.; Sokolov, N. I. *Synth. Met.*, in press.

(8) Mysyk, D. D.; Perepichka, I. F.; Perepichka, D. F.; Bryce, M. R.; Popov, A. F.; Goldenberg, L. M.; Moore, A. J. *J. Org. Chem.* **1999**, *64*, 6937.

(9) (a) Hoegl, H.; Barchietto, G.; Tar, D. *Photochem. Photobiol.* **1972**, *16*, 335. (b) Enomoto, T.; Hatano, M. *Makromol. Chem.* **1974**, *175*, 57. (c) Perepichka, I. F.; Mysyk, D. D.; Sokolov, N. I. In *Current Trends in Polymer Photochemistry*; Allen, N. S., Edge, M., Bellobono, I. R., Selli, E., Eds.; Ellis Horwood: New York, 1995; p 318. (d) Strohriegl, P.; Grazulevicius, J. V. In *Handbook of Organic Conductive Molecules and Polymers*; Nalwa, H. S., Ed.; Wiley: Chichester, U.K., 1997; Vol. 1, p 553.

(10) (a) Abramov, V. N.; Andrievskii, A. M.; Bodrova, N. A.; Borodkina, M. S.; Kravchenko, N. V.; Kostenko, L. I.; Malakhova, I. A.; Nikitina, E. G.; Orlov, I. G.; Perepichka, I. F.; Pototskii, I. S.; Semenenko, N. M.; Trushina, V. S. USSR Patent 1,343,760, 1987. (b) Mysyk, D. D.; Neilands, O. Ya.; Kuvshinsky, N. G.; Sokolov, N. I.; Kostenko, L. I. USSR Patent 1,443,366, 1987. (c) Belonozhko, A. M.; Davidenko, N. A.; Kuvshinsky, N. G.; Neilands, O. Ya.; Mysyk, D. D.; Prizva, G. I. USSR Patent 1,499,553, 1989. (d) Mysyk, D. D.; Neilands, O. Ya.; Khodorkovsky, V. Yu.; Kuvshinsky, N. G.; Belonozhko, A. M.; Davidenko, N. A. USSR Patent 1,665,-678, 1991. (e) Kuvshinskii, N. G.; Nakhodkin, N. G.; Davidenko, N. A.; Belonozhko, A. M.; Mysyk, D. D. *Ukr. Fiz. Zh.* **1989**, *34*, 1100 (in Russian). (f) Perepichka, I. F.; Mysyk, D. D.; Sokolov, N. I. *Synth. Met.* **1999**, *101*, 9.

(11) Perepichka, D. F.; Perepichka, I. F.; Bryce, M. R.; Popov, A. F.; Chesney, A.; Moore, A. J. In *Structures of Organic Compounds and Reaction Mechanisms*; Inst. Phys. Org., & Coal Chem.: Donetsk, Ukraine, 1998; p 94.

(12) Sariciftci, N. S.; Heeger, A. J. In *Handbook of Organic Conductive Molecules and Polymers*; Nalwa, H. S., Ed.; Wiley: Chichester, U.K., 1997; Vol. 1, p 413.

(13) (a) Da Ros, T.; Prato, M.; Guldi, D.; Alessio, E.; Ruzzi, M.; Pasimeni, L. *Chem. Commun.* **1999**, 635. (b) Pasimeni, L.; Maniero, A. L.; Ruzzi, M.; Prato, M.; Da Ros, T.; Barbarella, G.; Zambianchi, M. *Chem. Commun.* **1999**, 429.

(14) Konishi, T.; Sasaki, Y.; Fujitsuka, M.; Toba, Y.; Moriyama, H.; Ito, O. *J. Chem. Soc., Perkin Trans. 2* **1999**, 551. Simonsen, K. B.; Konovalov, V. V.; Konovalova, T. A.; Kawai, T.; Cava, M. P.; Kispert, L. D.; Metzger, R. M.; Becher, J. *J. Chem. Soc., Perkin Trans. 2* **1999**, 657. Liddell, P. A.; Kuciauskas, D.; Sumida, J. P.; Nash, B.; Nguyen, D.; Moore, A. L.; Moore, T. A.; Gust, D. *J. Am. Chem. Soc.* **1997**, *119*, 1400.

(15) Skabara, P. J.; Serebryakov, I. M.; Perepichka, I. F. *Synth. Met.* **1999**, *102*, 1336.

(16) (a) Abe, Y. *J. Chem. Soc. Jpn., Chem. Ind. Chem.* **1981**, 1966. (b) Andrievskii, A. M.; Sidorenko, E. N.; Titov, V. V.; Dyumaev, K. M. USSR Patent 982,322, 1982.

(17) (a) Perepichka, I. F.; Mysyk, D. D. USSR Patent 862,561, 1981. (b) Mysyk, D. D.; Perepichka, I. F.; Kostenko, L. I. USSR Patent 1,050,249, 1983.

(18) Jones, E.; Moodie, I. M. *J. Chem. Soc.* **1965**, 7018.

(19) Svenstrup, N.; Becher, J. *Synthesis* **1995**, 215.

(20) Miuaura, N.; Suzuki, A. *Chem. Rev.* **1995**, *96*, 2457 and references therein.

(21) Foa, M.; Santi, R.; Garavaglia, F. *J. Organomet. Chem.* **1981**, *26*, C29.

(22) Svenstrup, N.; Becher, J. *Synthesis* **1995**, 215.

(23) Gorgues, A.; Simon, A.; Le Coq, A.; Hercouet, A.; Corre, F. *Tetrahedron* **1986**, *42*, 351.

(24) Leriche, P.; Gorgues, A.; Jubault, M.; Becher, J.; Orduna, J.; Garin, J. *Tetrahedron Lett.* **1995**, *36*, 1275.

(25) Skabara, P. J.; Serebryakov, I. M.; Roberts, D. M.; Perepichka, I. F.; Coles, S. J.; Hursthouse, M. B. *J. Org. Chem.* **1999**, *64*, 6418.

(26) Hansch, C.; Leo, A.; Taft, R. W. *Chem. Rev.* **1991**, *91*, 165.

(27) Roncali, J. *Chem. Rev.* **1992**, *92*, 711.

(28) Orenstein, J. In *Handbook of Conducting Polymers*; Skotheim, T. A., Ed.; Marcel Dekker: New York, 1986; Chapter 36.

(29) Patil, A. O.; Heeger, A. J.; Wudl, F. *Chem. Rev.* **1988**, *88*, 183.

(30) See, for example: (a) Zerbi, G.; Gussoni, M.; Castiglioni, C. In *Conjugated Polymers*; Brédas, J. L., Silbey, R., Eds.; Kluwer: Dordrecht, The Netherlands, 1991; p 435. (b) Del Zoppo, M.; Castiglioni, C.; Zuliani, P.; Zerbi, G. In *Handbook of Conducting Polymers*, 2nd ed.; Skotheim, T. A., Reynolds, J. R., Eds.; Marcel Dekker: New York, 1988; Chapter 28 and references therein.

(31) (a) Horovitz, B. *Solid State Commun.* **1982**, *41*, 729. (b) Ehrenfreund, E.; Vardeny, Z. V.; Brafman, O.; Horovitz, B. *Phys. Rev. B* **1987**, *36*, 1535.

(32) Neugebauer, H.; Neckel, A.; Brinda-Konopik, N. In *Electronic Properties of Polymers and Related Compounds*; Kuzmany, H., Mehring, M., Roth, S., Eds.; Springer Series in Solid State Sciences, Springer: Berlin, 1985; Vol. 63, p 227.

(33) Tian, B.; Zerbi, G.; Mueller, K. *J. Chem. Phys.* **1991**, *95*, 3198.

(34) Gussoni, M.; Castiglioni, C.; Zerbi, G. In *Spectroscopy of Advanced Materials*; Clark, R. J. H., Hester, R. E., Eds.; Wiley: New York, 1991; p 251.

(35) (a) Neugebauer, H.; Nauer, G.; Neckel, A.; Tourillon, G.; Garnier, F.; Lang, P. *J. Phys. Chem.* **1984**, *88*, 652. (b) Neugebauer, H.; Ping, Z. *Mikrochim. Acta* **1997**, *[Suppl.] 14*, 125. (c) Neugebauer, H. *Macromol. Symp.* **1995**, *94*, 61. (d) Neugebauer, H.; Sariciftci, N. S. In *Lower Dimensional Systems and Molecular Electronics*; Metzger, R. M., Day, P., Papavassiliou, G. C., Eds.; Nato ASI Series; Series B: Physics; Plenum Press: New York, 1991; Vol. 248, p 251.

MA0015931